

## Heat capacity and thermodynamic properties of nearly stoichiometric wüstite from 13 to 450 K

SVEIN STØLEN,<sup>1</sup> RONNY GLÖCKNER,<sup>1</sup> FREDRIK GRØNVOLD,<sup>1</sup> TOORU ATAKE,<sup>2</sup> AND SATORU IZUMISAWA<sup>2</sup>

<sup>1</sup>Department of Chemistry, University of Oslo, P.O. Box 1033, Blindern, N-0315 Oslo, Norway

<sup>2</sup>Research Laboratory of Engineering Materials, Tokyo Institute of Technology, 4259 Nagatsuta-cho, Midori-ku, Yokohama, 226 Japan

### ABSTRACT

The heat capacity of a three-phase sample of  $\text{Fe}_{0.990 \pm 0.005}\text{O}$ ,  $\text{Fe}_3\text{O}_4$ , and Fe (mole fractions 0.915, 0.078, and 0.007, respectively) has been measured by adiabatic shield calorimetry at temperatures from 13 to 450 K.  $\text{Fe}_{0.99}\text{O}$  and magnetite are formed as a metastable intermediate on heating of a quenched nonstoichiometric wüstite with composition  $\text{Fe}_{0.9374}\text{O}$ . The small amount of Fe present stems from the second disproportionation reaction, in which the stable two-phase mixture of Fe and magnetite is formed from  $\text{Fe}_{0.99}\text{O}$ . The value of  $\Delta S_m$  ( $\text{Fe}_{0.99}\text{O}$ , 298.15 K), 60.45 J/(K·mol), is derived from the entropy of the three-phase sample and recommended standard entropies of Fe and magnetite. The character of the magnetic order-disorder transition changes with composition and is strongly cooperative in  $\text{Fe}_{0.99}\text{O}$ , with  $T_N \approx 191$  K. A minor, seemingly higher order transition is observed at  $\sim 124$  K. It is caused by the Verwey transition in the magnetite. This magnetite, formed in metastable equilibrium with  $\text{Fe}_{0.99}\text{O}$ , is presumably more Fe-rich than magnetite in stable equilibrium with Fe.

### INTRODUCTION

The typically nonstoichiometric iron monoxide, wüstite, probably participates in two reactions in the Earth's interior that are of geologic significance. In the boundary between the upper and lower mantle ( $T \approx 2750$  K,  $P \approx 24$  GPa) magnesiowüstite,  $(\text{Mg,Fe})\text{O}$ , and a magnesium-iron perovskite,  $(\text{Mg,Fe})\text{SiO}_3$ , are formed by disproportionation of the main component of the upper mantle,  $(\text{Mg,Fe})_2\text{SiO}_4$  (Liu 1975). Wüstite is presumably also formed in the so-called D" layer between the lower mantle and the inner liquid Fe core ( $T \approx 3500$  K,  $P \approx 136$  GPa). The presence of liquid iron diminishes the solubility of Fe in the perovskite-type silicate, resulting in the formation of wüstite (Knittle and Jeanloz 1989, 1991; Jeanloz 1990).

Although the compositional stability field of the grossly nonstoichiometric wüstite,  $\text{Fe}_{1-x}\text{O}$ , is sensitive to both temperature and pressure, details of the pressure-induced changes to the stability field are much disputed. Wüstite with composition  $\text{Fe}_{\sim 0.94}\text{O}$  forms eutectoidally from Fe and  $\text{Fe}_3\text{O}_4$ , magnetite, at  $\sim 835$  K at ambient pressure. The main effects of increased pressure up to  $\sim 10$  GPa are a decrease of the eutectoid temperature for wüstite formation and further extension of the wüstite phase field. Most reports conclude that the Fe-rich phase boundary of the  $\text{Fe}_{1-x}\text{O}$  phase approaches stoichiometry when pressure is increased to about 10 GPa:  $1 - x$  increases from 0.954 at ambient pressure and 1185 K to  $\sim 0.99$  at

10 GPa and  $\sim 600$  K (Fei and Saxena 1986). For higher pressures, our knowledge about the stability field of wüstite is uncertain. On the Fe-rich side increasing nonstoichiometry of wüstite is observed as pressure is increased (cf. Simons and Seifert 1979; Shen et al. 1983; McCammon and Liu 1984; McCammon 1993). At atmospheric pressure the O-rich phase boundary of  $\text{Fe}_{1-x}\text{O}$  moves toward higher O content as temperature is increased. The limiting value of  $1 - x$  is  $\sim 0.83$  at  $\sim 1700$  K. According to Shen et al. (1983) the trend with pressure is probably the same as for the Fe-rich phase boundary, i.e., at a given intermediate temperature the O-rich phase limit first moves in the direction of Fe, and then back as pressure is increased further. The high-pressure phase boundaries of wüstite, as derived from a thermodynamic description of the Fe-O system, are seen to depend markedly on assumptions regarding the compositional behavior of the bulk modulus of wüstite (Stølen and Grønvold, unpublished manuscript).

To derive the high-pressure properties and to model multicomponent phase diagrams involving wüstite, a thermodynamic description of the wüstite phase is needed that is also correct beyond the phase boundaries at ambient pressure. Two of the more recent evaluators of the voluminous literature on the thermodynamics of the Fe-O system differ with regard to the properties of the nonstoichiometric wüstite phase, especially for the metastable region near  $1 - x = 0.500$  (Sundman 1991; Haas and Hemingway 1992). The compositional variation of

the enthalpy of formation at 1075 K is shown together with experimental and estimated values in Figure 9 of Grønvold et al. (1993). In the same paper, molar heat capacities of stoichiometric FeO and of  $\text{Fe}_{0.90}\text{O}$  were estimated in the temperature range 300–1000 K from the results for  $\text{Fe}_{0.947}\text{O}$  (Coughlin et al. 1951; Todd and Bonnickson 1951) and  $\text{Fe}_{0.9379}\text{O}$  and  $\text{Fe}_{0.9254}\text{O}$  (Grønvold et al. 1993). For compositions approaching stoichiometry, the molar heat capacities in the 200–500 K region appear to be lower than for the more Fe-deficient samples, whereas the opposite, normal trend prevails at higher temperatures, 900–1000 K (Grønvold et al. 1993). This peculiarity was related to the more cooperative nature of the magnetic order-disorder process when stoichiometry was approached, an assumption that was qualitatively confirmed in a recent study of the decomposition of quenched wüstite (Stølen et al. 1995). On the basis of the chosen Gibbs energy of formation and the estimated heat capacity, the standard entropy of stoichiometric FeO at 298.15 K was estimated to be  $61 \pm 1 \text{ J}/(\text{K}\cdot\text{mol})$  (Grønvold et al. 1993). Haas and Hemingway (1992) derived a 4% larger value,  $63.46 \pm 0.71 \text{ J}/(\text{K}\cdot\text{mol})$  in his extensive thermodynamic analysis of the Fe-Si-O system, whereas Fei and Saxena (1986) gave a much lower value,  $57.59 \pm 0.20 \text{ J}/(\text{K}\cdot\text{mol})$ .

Nearly stoichiometric iron monoxide can be prepared as a metastable intermediate in a two-stage disproportionation of quenched metastable wüstite (Castelliz et al. 1954; Stølen et al. 1995). In the first stage an Fe-rich wüstite forms together with magnetite at  $\sim 450 \text{ K}$  and remains metastable to  $\sim 550 \text{ K}$ . At this temperature the stable two-phase mixture of Fe and magnetite slowly forms.

In the present study, the heat capacity of a three-phase mixture of  $\text{Fe}_{0.990 \pm 0.005}\text{O}$  ("Fe<sub>0.99</sub>O"),  $\text{Fe}_3\text{O}_4$ , and a small amount of Fe was determined over the temperature region 13–450 K. The sample was prepared through controlled disproportionation of a sample with composition  $\text{Fe}_{0.9374}\text{O}$  in a step-wise-heated adiabatic calorimeter. Careful monitoring of temperature-drift rates in the equilibration periods ensured optimum sample quality (see below). The composition of the Fe-rich intermediate and the ratio of the phases in the sample were derived from (1) the known variation of the lattice constant of wüstite with composition, (2) determination of the amount of magnetite in the sample through accurate determinations of the specific magnetic moment (the Fe content of the sample was also obtained from the compositions of the originally quenched and of the intermediately formed wüstite), and (3) refinement of the mole fractions of the different phases by Rietveld-type analysis of neutron diffraction results (Fjellvåg et al., unpublished data). The thermodynamic properties of  $\text{Fe}_{0.99}\text{O}$  are evaluated and discussed.

Magnetite is formed as a by-product in the first disproportionation step. Initially the enthalpy of the Verwey transition was believed to give a third estimate of the amount of magnetite contained in the sample. This esti-

mate was of less value because the enthalpy of the transition depends decisively on the stoichiometry of the phase.

## EXPERIMENTAL METHODS

### Sample preparation and characterization

The nonstoichiometric wüstite used in this investigation was prepared from ferric oxide and Fe. The  $\text{Fe}_2\text{O}_3$  (E. Merck no. 3294) was heated in alumina boats in an electric furnace at 1070 K until constant mass was attained. This required about 40 h and resulted in a mass loss of 0.05%. According to the manufacturer's analysis the impurity limits are (in percent by mass):  $\text{Cl}^-$  0.01;  $\text{SO}_4^{2-}$  0.01; N, Pb, Cu, Mg, Mn, Ni, Zn 0.005; insoluble in HCl 0.01. Spectrographic analysis also showed 50 ppm  $\text{SiO}_2$ . A small part of the sample was reduced to pure metallic iron with the use of dry  $\text{H}_2$  gas at 1120 K until the  $\text{Fe}_2\text{O}_3/\text{Fe}$  mass ratio was  $1.4295 \pm 0.0002$ , comparable to the theoretical value of 1.4297. Mixtures of this Fe and the  $\text{Fe}_2\text{O}_3$  in the nominal Fe/O ratio 0.94 were heated in evacuated and sealed vitreous silica tubes at 1270 K for 2 d and cooled in the furnace. Fifteen smaller samples with a total weight of 72 g were made. After crushing, the samples were reheated in evacuated vitreous silica tubes to 950 K for 3 d and quenched by being dropped into a solution of water, ice, and salt.

The O content of the calorimetric sample was determined by oxidation or reduction of 1.0–1.5 g samples at 1070 K in air or  $\text{H}_2$  to constant mass in alumina boats. The resulting O content of the samples corresponds to  $\text{Fe}_{0.9374}\text{O}$ . For further details see Grønvold et al. (1993).

Room-temperature X-ray diffraction patterns were taken with the Guinier-Hägg technique,  $\text{CrK}\alpha_1$  radiation, and Si as the internal calibration substance (Deslattes and Henins 1973). Magnetic measurements were performed with a SQUID quantum-design magnetic measurement system. The specific magnetic moments were calibrated using a standard platinum reference sample from NIST (NBS). The accuracy of the deduced specific moment is within 0.1%.

### Calorimetry

Details of the construction and measurement procedures for the laboratory-made, low-temperature calorimeter have been reported earlier (Atake et al. 1990). The mass of the sample loaded in the calorimeter was 22.8612 g or 0.33448 moles of  $\text{Fe}_{0.9374}\text{O}$ . The contribution of the sample to the total heat capacity of the calorimeter was about 25, 50, and 60% at 20, 100, and 300 K, respectively. Temperatures were measured with a platinum resistance thermometer calibrated at the National Physical Laboratory, U.K., on the basis of ITS-90.

The high-temperature calorimetric apparatus and measuring technique have been described earlier (Grønvold 1967, 1993). The calorimeter was step-wise heated and surrounded by electrically heated, electronically controlled adiabatic shields. The sample was enclosed in an

TABLE 1. Molar heat capacity of a sample with overall composition  $\text{Fe}_{0.9374}\text{O}$ 

$T$ (K)	$C_{p,m}$ [J/(K·mol)]	$T$ (K)	$C_{p,m}$ [J/(K·mol)]	$T$ (K)	$C_{p,m}$ [J/(K·mol)]	$T$ (K)	$C_{p,m}$ [J/(K·mol)]	$T$ (K)	$C_{p,m}$ [J/(K·mol)]	$T$ (K)	$C_{p,m}$ [J/(K·mol)]
<b>Series I*</b>											
313.02	49.95	122.938	31.82	224.848	41.55	75.532	13.14	159.384	38.83	248.902	42.75
319.80	50.11	125.111	31.60	227.130	41.64	77.618	13.77	161.044	39.21	251.221	42.86
326.55	50.13	127.359	30.56	229.405	41.75	79.629	14.38	162.689	39.74	253.533	42.95
333.26	50.29	129.685	30.28	231.673	41.85	81.574	14.96	164.316	40.39	255.875	43.09
339.96	50.37	132.030	30.59	233.934	41.97	83.459	15.53	165.924	41.08	258.247	43.21
346.66	50.28	134.287	31.16	236.188	42.07	85.290	16.09	167.512	41.84	260.611	43.33
353.35	50.24	136.452	31.79	238.435	42.19	87.070	16.63	169.122	42.67	262.968	43.44
359.98	50.69	138.640	32.49	240.675	42.31	88.806	17.16	170.794	43.60	265.319	43.56
366.60	50.84	140.850	33.23	242.908	42.43	90.501	17.67	172.540	44.68	267.663	43.70
373.22	51.08	143.023	34.00	245.134	42.44	92.159	18.18	174.334	45.94	270.000	43.80
380.63	50.86	145.161	34.81	247.354	42.65	93.781	18.67	176.117	47.38	272.331	43.92
392.82	51.01	147.262	35.64	249.567	42.78	95.370	19.15	177.860	49.02	274.655	44.03
401.23	51.14	149.328	36.49			96.929	19.63	179.561	50.95	276.974	44.14
409.69	51.23	151.359	37.33	<b>Series IV†</b>		98.458	20.10	181.214	53.23	279.285	44.24
418.19	51.32	153.359	38.07	11.441	0.093	99.960	20.57	182.836	55.98	281.591	44.35
426.73	51.41	155.336	38.49	12.445	0.085	101.437	21.02	184.423	59.01	283.891	44.46
435.32	51.63	157.300	38.64	13.715	0.111	103.018	21.52	185.957	61.62	286.191	44.55
443.95	51.70	159.254	38.82	15.198	0.154	103.350	21.63	187.433	65.62	288.475	44.66
453.19	51.88	161.195	39.26	16.748	0.208	105.268	22.23	188.804	76.03	290.752	44.77
461.88	52.11	163.116	39.91	18.215	0.269	107.145	22.84	189.968	102.42	293.023	44.85
471.01	52.25	165.012	40.69	19.655	0.344	108.983	23.47	190.782	196.14	295.290	44.94
		166.933	41.57	21.196	0.441	110.807	24.09	191.419	169.74	297.550	45.05
		168.930	42.57	22.864	0.567	112.639	24.74	192.265	104.56	299.805	45.15
		171.006	43.73	24.589	0.721	114.414	25.40	193.399	79.36		
		173.100	45.07	26.347	0.906	116.110	26.11	194.739	66.25	<b>Series V‡</b>	
		175.209	46.63	28.090	1.117	117.772	26.95	196.234	58.04	185.146	59.77
		177.327	48.50	29.846	1.357	119.396	28.03	197.850	52.55	186.162	61.55
		179.415	50.78	31.640	1.631	120.970	29.66	199.557	48.83	187.240	64.68
		181.493	53.69	33.408	1.928	122.487	31.52	201.332	46.31	188.265	70.83
		183.547	57.34	35.183	2.253	123.965	32.10	203.268	44.52	189.203	82.58
		185.544	60.93	36.994	2.608	125.440	31.41	205.354	43.26	190.007	107.14
		187.501	66.19	38.846	2.996	126.931	30.67	207.467	42.45	190.503	151.88
		189.323	85.11	40.721	3.410	128.450	30.30	209.596	41.94	190.746	197.26
		190.648	174.11	42.587	3.844	129.990	30.27	211.735	41.63	190.955	210.50
		191.669	143.11	44.432	4.290	131.541	30.47	213.878	41.44	191.172	183.04
		193.011	86.06	46.274	4.752	133.099	30.82	216.021	41.38	191.422	152.52
		194.795	66.06	48.116	5.225	134.701	31.26	218.163	41.40	191.712	127.94
		196.870	55.66	49.990	5.721	136.402	31.77	220.301	41.41	192.045	109.94
		199.150	49.63	51.895	6.235	138.231	32.35	222.435	41.46	192.417	97.03
		201.567	46.08	53.769	6.752	140.126	32.97	224.564	41.53	192.823	87.55
		204.072	43.98	55.633	7.274	141.994	33.62	226.687	41.62	193.259	80.34
		206.479	42.79	57.526	7.811	143.836	34.29	228.805	41.72	193.722	74.62
		208.762	42.11	59.454	8.364	145.652	34.98	230.917	41.82	194.209	69.96
		211.060	41.70	61.374	8.922	147.442	35.69	233.023	41.92	194.718	66.01
		213.364	41.48	63.296	9.484	149.205	36.43	235.188	42.03	195.247	62.66
		215.668	41.39	65.227	10.05	150.943	37.15	237.410	42.14	195.794	59.78
		217.970	41.40	67.180	10.63	152.659	37.82	239.660	42.26		
		220.269	41.41	69.159	11.22	154.355	38.30	241.937	42.38		
		222.560	41.47	71.201	11.83	156.039	38.55	244.242	42.49		
				73.361	12.48	157.715	38.64	246.576	42.61		

Note:  $M(\text{Fe}_{0.9374}\text{O}) = 68.3504$  g/mol.

\* As-quenched sample, University of Oslo.

\*\* Partially disproportionated sample, University of Oslo.

† Partially disproportionated sample, Tokyo Institute of Technology.

evacuated and sealed vitreous silica tube of about 50 cm<sup>3</sup> volume. A central well in the tube contained the heater and platinum resistance thermometer. The thermometer was calibrated locally at the ice, steam, tin, zinc, and antimony points according to IPTS-68. The temperatures were subsequently converted to ITS-90 and are judged to correspond to ITS-90 within 0.05 K up to 900 K and within 0.10 K above 900 K. The resistance was measured with an ASL F-18 resistance bridge. The heat capacity of the ~70 g sample represents about 25% of the total heat capacity of the calorimeter. The relatively small amount of sample used in the present investigation degraded the

usual accuracy obtained with this apparatus ( $\pm 0.25\%$ ) to  $\pm 0.5\%$ . The heat capacity of the empty calorimeter was determined in a separate series of experiments.

## RESULTS AND DISCUSSION

The heat-capacity data for the quenched wüstite,  $\text{Fe}_{0.9374}\text{O}$ , are given in Table 1 and plotted for one mole of atoms as a function of temperature in Figure 1 (solid circles). The dotted and solid lines in the figure represent the heat capacity of the two-phase mixtures of  $\text{Fe} + \text{Fe}_3\text{O}_4$  and  $\text{FeO} + \text{Fe}_3\text{O}_4$ , respectively, calculated for the overall composition  $\text{Fe}_{0.9374}\text{O}$ . Heat-capacity values for FeO and

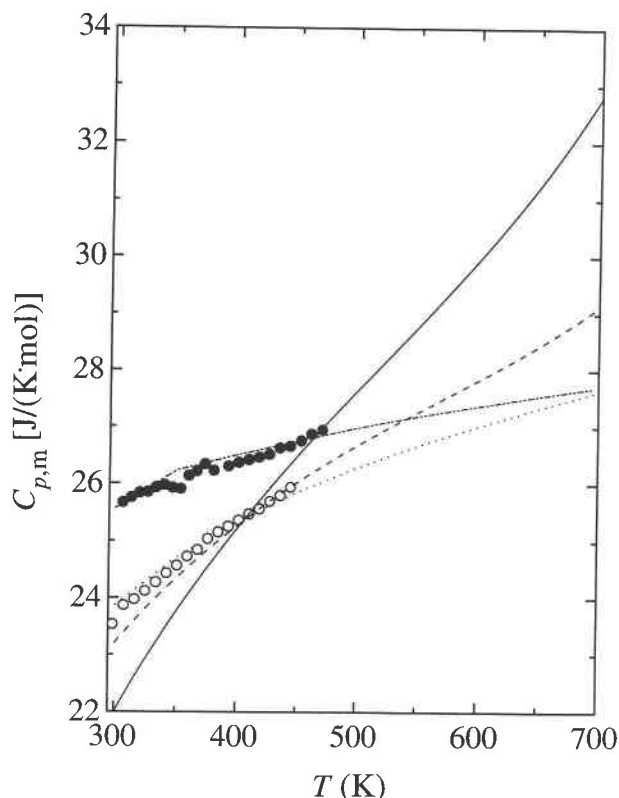


**FIGURE 1.** Molar heat capacity of  $(1/1.9374)\text{Fe}_{0.9374}\text{O}$ . Solid circles = University of Oslo (UO) results for quenched wüstite; open circles = UO results for the partially disproportionated sample. The heat capacities of the two-phase mixture of  $\text{Fe} + \text{Fe}_3\text{O}_4$  and  $\text{FeO} + \text{Fe}_3\text{O}_4$ , calculated for the overall composition  $\text{Fe}_{0.9374}\text{O}$ , are represented by solid and dashed lines, respectively. The dotted and dash-dot lines represent equations for  $(1/1.9427)\text{Fe}_{0.9247}\text{O}$  and  $(1/2)\text{FeO}$ , respectively (Grønvdal et al. 1993).

$\text{Fe}_3\text{O}_4$  are from Grønvdal et al. (1993), whereas those for Fe are from Haas and Hemingway (1992). Near 470 K positive temperature-drift rates, which indicate the onset of the first disproportionation step in the two-stage disproportionation reaction, were observed in the equilibration periods. The calorimetric experiments were continued until the instrumental temperature-drift rate was almost regained (at  $\sim 535$  K), after which the sample was cooled in the furnace to ambient temperature. A “two-phase” specimen (see below) of  $\text{Fe}_{0.99}\text{O}$  and  $\text{Fe}_3\text{O}_4$ , magnetite, was thus prepared in the calorimeter by careful disproportionation of the quenched metastable wüstite.

In a second series of experiments, the heat capacity of the intermediately formed two-phase specimen was determined in the temperature range 300–440 K, after which low-temperature experiments were performed. The heat capacities are presented in Figures 1 (open circles) and 2, and the experimental results are also given in chronologic order in Table 1. Two distinct phase transitions are observed at 124 and 191 K, respectively. The heat-capacity

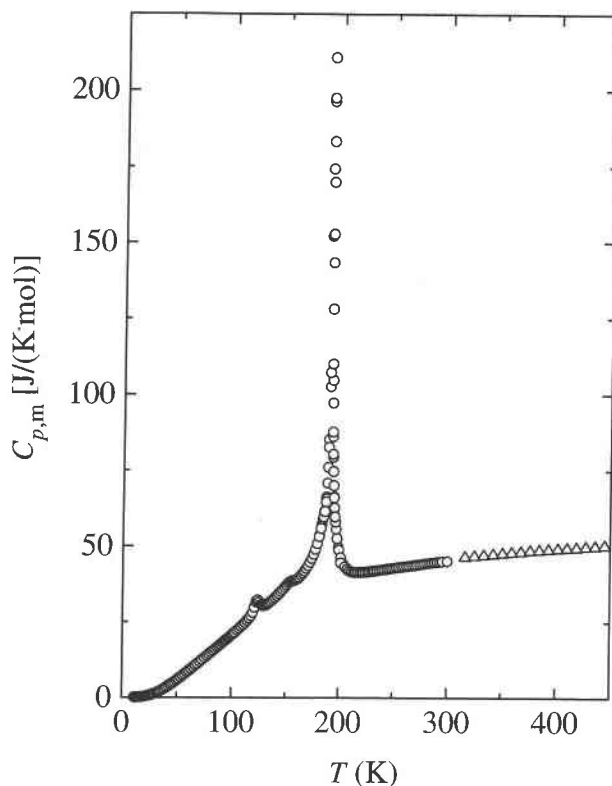


**FIGURE 2.** Molar heat capacity of  $(1/1.9374)\text{Fe}_{0.9374}\text{O}$ . Open circles = Tokyo Institute of Technology results; open triangles = University of Oslo results.

effect connected with the magnetic order-disorder transition in the Fe-rich wüstite at 191 K is typical of a higher-order transition, whereas the effect at 124 K is caused by the Verwey transition in the magnetite present. An anomalous shoulder on the heat-capacity curve at  $\sim 160$  K is of less certain origin.

The lattice constants of the initially quenched wüstite, of the products of the first disproportionation reaction (the present sample), and of the stable two-phase mixture,  $\text{Fe} + \text{Fe}_3\text{O}_4$ , are given in Table 2. In addition to the reflections from  $\text{Fe}_{0.99}\text{O}$  and magnetite, one very weak reflection corresponding to the strongest reflection from Fe was detected by X-ray diffraction. All lines from the initial phase with  $a = 430.4 \pm 0.2$  pm were absent. Thus, the sample went through the first disproportionation stage and the second reaction began before the sample was brought to room temperature. Still, this method is judged to represent the best controllable method for preparation of a nearly pure two-phase sample in the presence of two disproportionation reactions that take place simultaneously.

It has been shown that the relationship between lattice constant and composition of wüstite, expressed as  $x_{\text{O}}$ , is approximately linear (see, e.g., Grønvdal et al. 1993). The lattice constant observed for  $\text{Fe}_{0.99}\text{O}$ ,  $a = 432.6 \pm 0.2$  pm, corresponds to an Fe/O ratio of 0.99 with the as-

**TABLE 2.** Lattice constants of the different phases observed after different thermal treatments

Phase	Lattice constant (pm)
<b>Prepared</b>	
Fe <sub>0.9374</sub> O	430.4 ± 0.2
<b>After first disproportionation step</b>	
"FeO"	432.6 ± 0.2
Fe <sub>3</sub> O <sub>4</sub>	840.5 ± 0.2
Fe	one very weak line
<b>After second disproportionation step</b>	
Fe	present
Fe <sub>3</sub> O <sub>4</sub>	839.5 ± 0.2

sumption that the lattice constant of stoichiometric FeO is 433.0 pm. The uncertainty in the Fe/O ratio is relatively large, probably about ±0.005.

With knowledge of the composition of the initially quenched specimen, Fe<sub>0.9374</sub>O, and of the intermediately formed wüstite, the amounts of Fe and magnetite in the three-phase sample were determined from measurement of the specific magnetic moment of the sample at 4 K and magnetic field strength up to 4 MA/m. By extrapolation of these results to a magnetic field of zero, the specific magnetic moment was found to be 22.3 (A·m<sup>2</sup>)/g. The values of the specific magnetic moment of magnetite and Fe are from Stølen et al. (1995) and Danan et al. (1968) and gave the following weight percentages for Fe<sub>0.99</sub>O, Fe<sub>3</sub>O<sub>4</sub>, and Fe; 78.43, 21.00, and 0.57, respectively. A closely concordant phase distribution was obtained from neutron diffraction results: 77.72, 21.90, 0.38 (cf. Fjellvåg et al., unpublished manuscript). In the following discussion, the averages of the two sets of values are used, i.e., 78.08, 21.45, and 0.48 wt%, which correspond to the mole fractions 0.915, 0.078, and 0.007 of Fe<sub>0.99</sub>O, Fe<sub>3</sub>O<sub>4</sub>, and Fe, respectively.

#### Heat capacity and thermodynamic properties of Fe<sub>0.99</sub>O

With the above distribution of phases in our calorimetric sample, heat-capacity values for Fe<sub>0.99</sub>O can be derived. In the evaluation, the low-temperature heat capacities of Fe<sub>3</sub>O<sub>4</sub> and Fe were taken from Takai et al. (1994b) and Desai (1986), whereas the values above ambient temperature were taken from Grønvold et al. (1993) and Haas and Hemingway (1992), respectively. The heat capacity of Fe<sub>0.99</sub>O is presented in Figure 3 together with those for three nonstoichiometric wüstite samples. The molar heat capacity of wüstite, given as  $[1/(2-x)]\text{Fe}_{1-x}\text{O}$ , varies considerably with composition above the Néel temperature. Earlier reported experimental and estimated heat capacities for wüstite in the temperature range 300–500 K are shown in Figure 4. The heat capacity of (1/1.99)Fe<sub>0.99</sub>O is approximately 7% lower than that of (1/1.9254)Fe<sub>0.9254</sub>O at 300 K.

The low heat-capacity values for Fe<sub>0.99</sub>O above the Néel temperature reflect the more strongly cooperative nature of the magnetic order-disorder transition in wüstite as stoichiometry is approached. This behavior is presu-

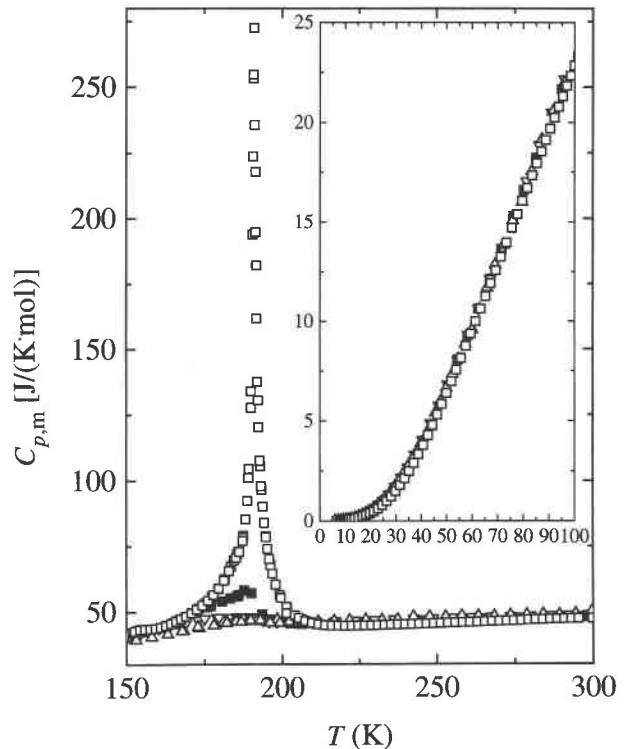


**FIGURE 3.** Molar heat capacities of quenched wüstite from 5 to 300 K. Open triangles = Fe<sub>0.9254</sub>O (Grønvold et al. 1993); open inverted triangles = Fe<sub>0.9379</sub>O (Grønvold et al. 1993); solid squares = Fe<sub>0.947</sub>O (Todd and Bonnicksen 1951); open squares = present results.

ably associated with the changing concentration of atomic defects and defect clusters and is strongly related to the degree of nonstoichiometry (Schweika et al. 1995). The complex defect clusters in grossly nonstoichiometric wüstite constitute magnetically coupled entities, which weaken the cooperative magnetic order-disorder behavior and cause the transition to be spread over a wide temperature range. This view is supported by the large magnetic moment observed for Fe<sub>0.99</sub>O (Fjellvåg et al., unpublished manuscript), which indicates that the number of defect clusters decreases as stoichiometry is approached.

The previous heat-capacity estimates for FeO by Grønvold et al. (1993) agree well with the present experimental values for Fe<sub>0.99</sub>O, whereas estimates by Haas and Hemingway (1992), and especially by Fei and Saxena (1986), are too large. Sundman's (1991) assessed heat-capacity values for Fe<sub>0.947</sub>O agree at 300 K but are about 4% low at 500 K.

The heat capacity of the intermediately formed three-phase sample was fitted to polynomials in temperature and integrated to give values for the thermodynamic functions at selected temperatures (see Table 3). Thermodynamic values for Fe<sub>0.99</sub>O were obtained after subtraction of the contributions of Fe [obtained by integration of the heat capacities recommended by Desai (1986)]

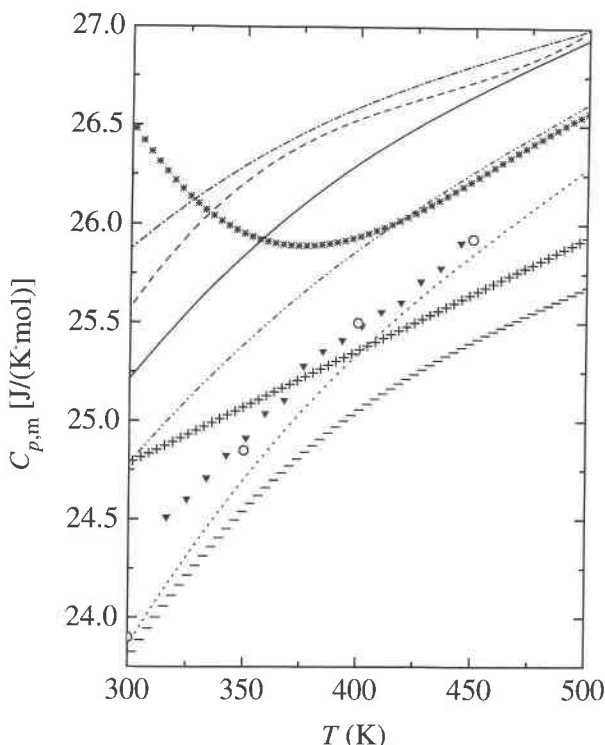


**FIGURE 4.** Molar heat capacities of quenched wüstite from 300 to 500 K. Solid inverted triangles = present experimental results for  $(1/1.99)\text{Fe}_{0.99}\text{O}$ ; open circles = presently recommended values for  $(1/1.99)\text{Fe}_{0.99}\text{O}$ . Dash-dot line = equation for  $(1/1.9254)\text{Fe}_{0.9254}\text{O}$ ; solid line = equation for  $(1/1.9379)\text{Fe}_{0.9379}\text{O}$ ; dotted line = equation for  $(1/2)\text{FeO}$  (Grønvold et al. 1993); dash-dot-dotted line = results for  $(1/1.947)\text{Fe}_{0.947}\text{O}$  (Todd and Bonnickson 1951); asterisks = equation for  $(1/2)\text{FeO}$  (Fei and Saxena 1986); plus signs = equation for  $(1/1.947)\text{Fe}_{0.947}\text{O}$  (Sundman 1991); bars = equation for  $(1/2)\text{FeO}$  (Haas and Hemingway 1992).

and magnetite (Takai et al. 1994b) and are given for selected temperatures in Table 4.

Previously reported experimental and estimated values of the standard entropy at 298.15 K are shown in Figure 5. The present value for  $\text{Fe}_{0.99}\text{O}$ , 60.45 J/(K·mol), agrees with that estimated for FeO by Grønvold et al. (1993),  $61 \pm 1$  J/(K·mol). The main uncertainty in the present evaluation relates to the composition of the nearly stoichiometric wüstite. A relatively large uncertainty in the composition,  $\pm 0.005$ , is reasonable because the composition is derived from the value of the lattice constant of the wüstite phase. A measure of the error in entropy induced by an incorrect composition of the nearly stoichiometric phase may be obtained by recalculating the standard molar entropy of wüstite, assuming it to be stoichiometric FeO. The resulting value is  $\Delta S_m(\text{FeO}, 298.15 \text{ K}) = 60.9$  J/(K·mol). Thus,  $\Delta S_m(\text{FeO}, 298.15 \text{ K}) = 61 \pm 1$  J/(K·mol) remains a reasonable estimate. The standard molar entropy estimated by Haas and Hemingway (1992) is 4% larger, the one by Fei and Saxena (1986)

**TABLE 3.** Molar thermodynamic properties of the sample with overall composition  $\text{Fe}_{0.9347}\text{O}$

$T$ (K)	$C_{p,m}$ [J/(K·mol)]	$\Delta_f^{\circ}H_m$ (J/mol)	$\Delta_f^{\circ}S_m$ [J/(K·mol)]	$\phi_m^{\circ}(T,0)$ [J/(K·mol)]
10	0.05	0.18	0.03	0.012
15	0.15	0.63	0.07	0.028
20	0.36	1.85	0.14	0.048
25	0.76	4.58	0.26	0.077
30	1.38	9.84	0.45	0.122
35	2.22	18.76	0.72	0.184
40	3.25	32.35	1.08	0.271
45	4.43	51.49	1.53	0.386
50	5.73	76.84	2.06	0.523
60	8.52	147.90	3.35	0.885
70	11.46	247.76	4.88	1.341
80	14.48	377.49	6.61	1.891
90	17.51	537.47	8.49	2.518
100	20.53	727.71	10.49	3.213
110	23.80	949.36	12.60	3.969
120	28.64	1207.4	14.85	4.788
130	30.28	1532.8	17.45	5.659
140	32.93	1846.9	19.78	6.588
150	36.76	2194.7	22.18	7.549
160	38.90	2576.4	24.64	8.538
170	43.10	2984.2	27.11	9.556
180	51.39	3451.8	29.78	10.60
191	(230)	(4239.2)	(34.01)	(11.82)
200	48.27	4906.2	37.44	12.91
210	41.85	5345.4	39.58	14.13
220	41.42	5760.5	41.51	15.33
230	41.76	6176.0	43.36	16.51
240	42.27	6600.0	45.16	17.66
250	42.77	7025.2	46.90	18.80
260	43.28	7455.5	48.58	19.91
270	43.79	7890.8	50.23	21.01
280	44.30	8331.3	51.83	22.08
290	44.81	8776.8	53.39	23.13
298.15	45.18	9136.2	54.64	24.00
300	45.31	9227.4	54.92	24.16
350	47.58	11552	62.08	29.07
400	49.26	13976	68.55	33.61
450	50.35	16464	74.41	37.82

Note:  $M(\text{Fe}_{0.9374}\text{O}) = 68.3504$  g/mol.

is 5.5% lower, and the one by Sundman (1991) is 2.5% lower. The previously estimated thermodynamic properties of stoichiometric FeO (Grønvold et al. 1993) are retained here.

The present thermodynamic values for FeO differ considerably from existing estimates and may prove useful in the important task of extending the thermodynamic description of the Fe-O system to high pressure.

**TABLE 4.** Molar thermodynamic properties of  $\text{Fe}_{0.99}\text{O}$

$T$ (K)	$C_{p,m}$ [J/(K·mol)]	$\Delta_f^{\circ}H_m$ (J/mol)	$\Delta_f^{\circ}S_m$ [J/(K·mol)]	$\phi_m^{\circ}(T,0)$ [J/(K·mol)]
50	6.40	85.45	2.29	0.581
100	22.81	811.2	11.70	3.588
150	41.26	2385.5	24.24	8.337
200	54.48	5558.9	42.05	14.26
250	45.47	7846.2	52.28	20.90
298.15	47.43	10073	60.45	26.66
300	47.56	10170	60.74	26.84
350	49.45	12574	68.21	32.28
400	50.75	15082	74.88	37.18
450	51.59	17636	80.89	41.70

Note:  $M(\text{Fe}_{0.99}\text{O}) = 71.28793$  g/mol.

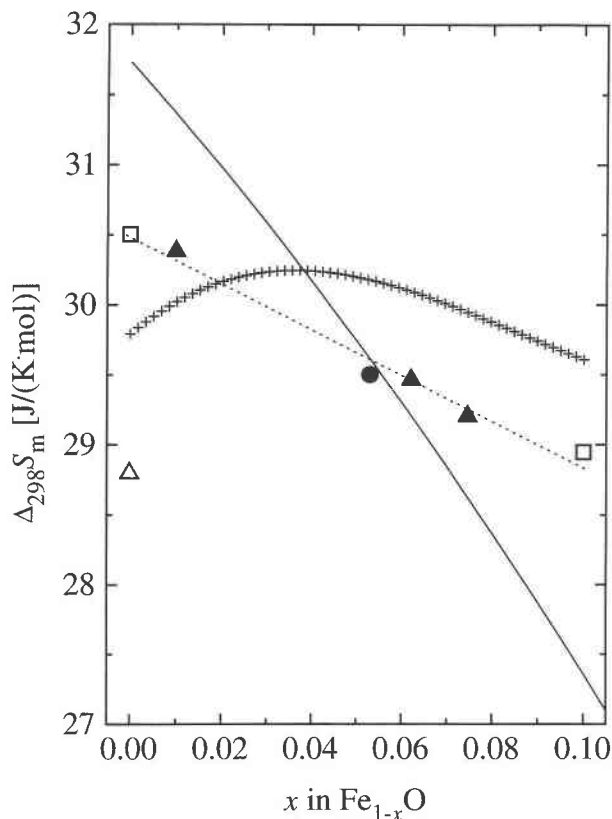


**FIGURE 5.** Standard entropy of wüstite at 298.15 K. Solid triangles = experimental results for  $(1/1.9254)\text{Fe}_{0.9254}\text{O}$ ,  $(1/1.9379)\text{Fe}_{0.9379}\text{O}$  (Grønvdal et al. 1993), and  $(1.199)\text{Fe}_{0.99}\text{O}$  (present study); open squares = estimated values for  $(1/2)\text{FeO}$  and  $(1/1.90)\text{Fe}_{0.90}\text{O}$  (Grønvdal et al. 1993); solid circle = experimental value for  $(1/1.947)\text{Fe}_{0.947}\text{O}$  (Todd and Bonnicksen 1951); open triangle = estimated value for  $(1/2)\text{FeO}$  (Fei and Saxena 1986); solid line = equation given by Haas and Hemingway (1992); plus signs = equation given by Sundman (1991); dotted line = compositional variation recommended here.

### The magnetic order-disorder transition

The present study shows that the magnetic order-disorder transition in  $\text{Fe}_{0.99}\text{O}$  is much more cooperative than earlier observed for wüstite with composition further from stoichiometry (Todd and Bonnicksen 1951; Grønvdal et al. 1993). To derive an estimate of the transitional entropy, a nonmagnetic reference molar heat capacity for  $\text{Fe}_{0.99}\text{O}$  has to be subtracted. Two alternative Debye-type background curves were derived after subtracting a dilatational heat-capacity contribution from the observed  $C_p$  results. In one approach, a constant Debye temperature was used with  $\theta_D = 430$  K, as obtained from the maximum in a plot of  $\theta_D$  vs. temperature. Another reference heat-capacity curve was obtained with a linear decrease in Debye temperature from 430 K at 100 K to 350 K at 260 K, where the cooperative part of the transition seems negligible. The reference heat capacities are shown in Figure 6 together with the heat capacities of different wüstite samples in the temperature region 100–300 K. The molar

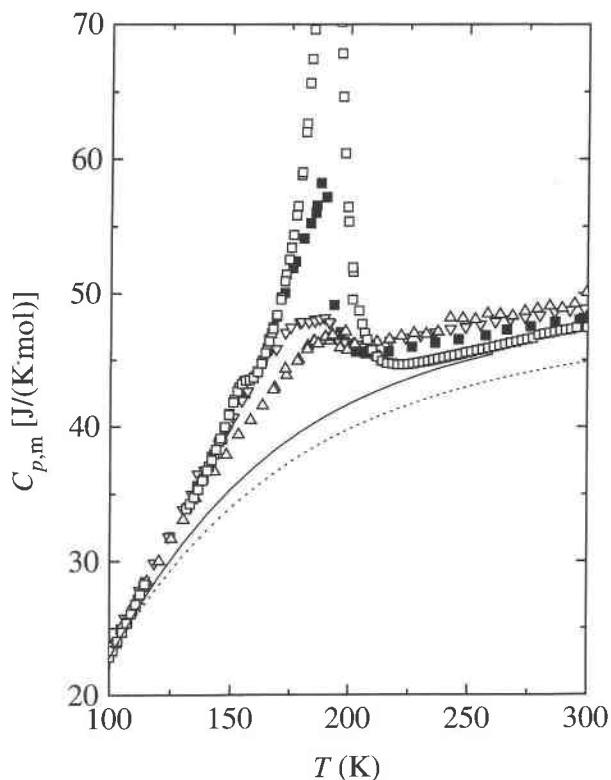


**FIGURE 6.** Molar heat capacities of quenched wüstite near  $T_N$ . Open triangles =  $\text{Fe}_{0.9254}\text{O}$  (Grønvdal et al. 1993); open inverted triangles =  $\text{Fe}_{0.9379}\text{O}$  (Grønvdal et al. 1993); solid squares =  $\text{Fe}_{0.947}\text{O}$  (Todd and Bonnicksen 1951); open squares = present results. The dotted and solid lines represent background estimates using  $\theta_D = 430$  K and a variable  $\theta_D$ , respectively (see text).

magnetic entropy is only 7.73 J/(K·mol) if the latter reference heat capacity is used. The assumption of  $\theta_D = 430$  K above 100 K leads to  $\Delta_{\text{mag}}S_m = 9.55$  J/(K·mol) at 300 K and implies the presence of additional magnetic heat-capacity contributions at higher temperatures. Furthermore, the assumption of negligible magnetic contributions to the heat capacity at temperatures below 100 K may be an oversimplification. A final conclusion has to await additional experiments and calculations of the phonon and magnon contributions to the heat capacity of wüstite. The expected spin-only magnetic entropy increment,  $\Delta_{\text{mag}}S_m = 0.99R \ln 5 = 13.38$  J/(K·mol), still has not been reached.

The Néel temperature, as observed by adiabatic calorimetry, does not vary significantly with composition, even though the concentration of defect clusters, and thus the cooperative nature of the transition, vary considerably.  $T_N = 189$  K was observed for  $\text{Fe}_{0.947}\text{O}$  (Coughlin et al. 1951) and  $\text{Fe}_{0.9379}\text{O}$ , and 193 K for  $\text{Fe}_{0.9254}\text{O}$  (Grønvdal et al. 1993), whereas the presently observed Néel temperature is 191 K.

Investigators have previously reported variation of the Néel temperature with composition. According to Koch



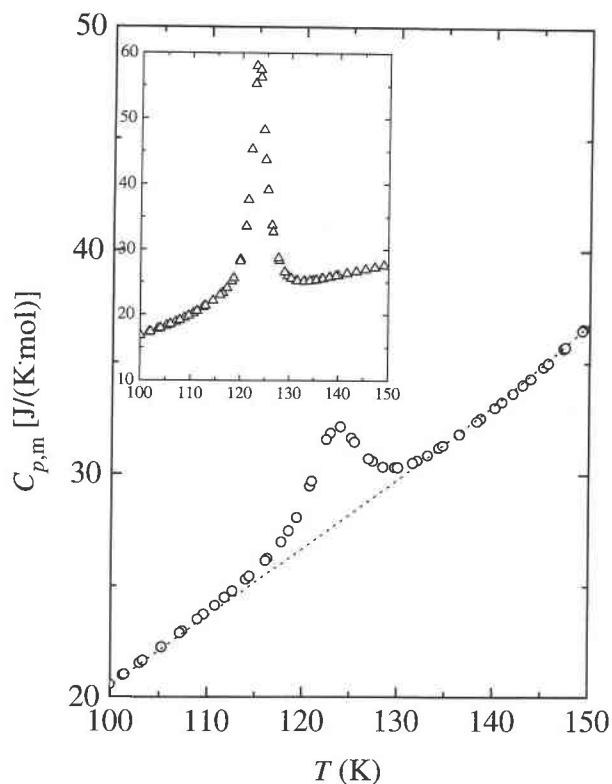


**FIGURE 7.** Molar heat capacity of the partially disproportionated sample near  $T_{\text{Verwey}}$ . Corresponding data for the fully disproportionated sample are shown in the inset. Dashed line represents estimated nontransitional heat capacity.

and Fine (1967) and Seehra and Srinivasan (1984) the Néel temperature decreases with increasing Fe content. The opposite variation was reported by Mainard et al. (1968), whereas McCammon (1992) reported that  $T_N$  decreases from 210 K for  $\text{Fe}_{0.90}\text{O}$  to 192 K for  $\text{Fe}_{0.95}\text{O}$ , and then  $T_N$  increases to 202 K for  $\text{Fe}_{0.98}\text{O}$ . The discrepancy between the different studies indicates that the magnetic properties of quenched wüstite may be affected by the thermal history, through differences in type and amount of the frozen-in defects. Such differences are, however, not expected to influence the thermodynamic properties of wüstite within the present accuracy of measurement.

#### Higher order Verwey transition in Fe-rich metastable magnetite

According to Dieckmann (1982), the composition of magnetite exceeds the stoichiometric 3:4 ratio in equilibrium with hematite,  $\text{Fe}_2\text{O}_3$ , at high temperatures. Below the eutectoid decomposition temperature of wüstite, magnetite appears to be stoichiometric in equilibrium with Fe. Because the magnetite in the present study was formed in metastable equilibrium with  $\text{Fe}_{0.99}\text{O}$ , and not in stable equilibrium with Fe, we suggest that a more Fe-rich magnetite is formed because a metastable phase generally increases the stability fields of the neighboring phase or phases. It has been reported that magnetite with excess

Fe can be obtained by low-temperature  $\text{H}_2$  reduction of  $\text{Fe}_3\text{O}_4$  (Colombo et al. 1967). The formation of an Fe-rich magnetite is in the present case indicated by the large lattice constant of magnetite obtained after the first disproportionation reaction [in agreement with Colombo et al. (1967)]. The lattice constant decreases from  $840.5 \pm 0.2$  to  $839.5 \pm 0.2$  pm, which is typical for stoichiometric magnetite, after further annealing, wherein the stable two-phase mixture of Fe and magnetite is obtained (Table 2).

The heat capacity of the ( $\text{Fe}_{0.99}\text{O} + \text{Fe}_3\text{O}_4 + \text{Fe}$ ) sample near the Verwey transition is shown in Figure 7. The broad heat-capacity effect does not accord with the discontinuity expected from earlier studies that indicate the Verwey transition to be of first order for nearly stoichiometric  $\text{Fe}_{3(1-\delta)}\text{O}_4$  (Shepherd et al. 1991; Takai et al. 1994a). The transition becomes second order when  $\delta > 0.004$  and then occurs at appreciably lower temperatures. The magnetite presently obtained in the disproportionation reaction is thus nearly stoichiometric and probably slightly Fe-rich. The nature of the Verwey transition in such Fe-rich magnetite is not known. It may be of higher order and occur at a relatively high temperature. To study this phenomenon further, the calorimetric sample was annealed at 500 K for 3 weeks and thereby converted to the stable two-phase mixture of Fe and magnetite. The heat capacity of this product is shown in the inset of Figure 7 (the absolute value of the heat capacity is uncertain because the sample contained a small amount of glass after accidental breakage of the sample container during transport). The transition is somewhat more cooperative, but not of first order as expected for stoichiometric  $\text{Fe}_3\text{O}_4$ . The sharpening of the heat-capacity peak accompanying the Verwey transition cannot unequivocally be ascribed to a change in the composition of the magnetite. It may equally well represent an annealing effect, with broadening of the peak owing to a distribution of magnetite grains with slightly differing compositions.

The entropy of the first-order Verwey transition for nearly stoichiometric  $\text{Fe}_{3-\delta}\text{O}_4$  varies from 6.0 J/(K·mol) for  $\delta = -0.0002$  to 4.0 J/(K·mol) for  $\delta = 0.0035$ . The Verwey transition is of higher order for the more O-rich magnetite, and the entropy of transition is much lower, e.g., 1.8 J/(K·mol) for  $\delta = 0.004$ . Thus, the enthalpy value of the Verwey transition cannot be used for accurate determination of the amount of magnetite present in the ( $\text{Fe}_{0.99}\text{O} + \text{Fe}_3\text{O}_4 + \text{Fe}$ ) sample. Integration of the excess heat capacity, shown in Figure 7, leads to the entropy 4.0 J/(K·mol) for the Verwey transition in  $\text{Fe}_3\text{O}_4$ . The entropy equals that observed for the first-order transition for  $\text{Fe}_{3-\delta}\text{O}_4$ , with  $\delta = 0.0035$ , and hence indicates a nearly stoichiometric composition for the magnetite studied here.

The origin of the shoulder on the heat-capacity curve near 150 K is uncertain. It is probably not related to the Verwey transition in the magnetite. If so, the molar entropy of transition becomes 10.2 J/(K·mol) of  $\text{Fe}_3\text{O}_4$ . This value is improbably high in comparison with earlier reported values. Thus, the shoulder is tentatively ascribed to the wüstite phase.



In conclusion, the magnetite formed in metastable equilibrium with  $\text{Fe}_{0.99}\text{O}$  is probably Fe rich. It is probably burdened by local fluctuations in composition. The preparation method may, however, provide new means for studying the nature of the Verwey transition. Such magnetite is presumably more Fe rich than  $\text{Fe}_{3\pm 6}\text{O}_4$  in equilibrium with Fe. Further calorimetric results might thus shed light on the ongoing discussion about the changes in the Verwey transition properties of magnetite with O deficiency and surplus (see, e.g., Shepherd et al. 1991; Takai et al. 1994a).

## REFERENCES CITED

- Atake, T., Kawaji, H., Hamano, A., and Saito, Y. (1990) Construction of an adiabatic calorimeter for heat capacity measurements from liquid helium temperatures to 330 K. Report of the Research Laboratory of Engineering Materials, Tokyo Institute of Technology, 15, 13–23.
- Castelliz, L., de Sutter, W., and Halla, F. (1954) On the decomposition of the wüstite phase. *Monatshefte für Chemie*, 85, 487–490 (in German).
- Colombo, U., Gazzarrini, F., and Lanzavecchia, G. (1967) Mechanism of iron oxides reduction at temperatures below 400 °C. *Materials Science and Engineering*, 2, 125–135.
- Coughlin, J.P., King, E.G., and Bonnicksen, K.R. (1951) High temperature heat content of ferrous oxide, magnetite and ferric oxide. *Journal of the American Chemical Society*, 73, 3891–3893.
- Danan, H., Herr, A., and Meyer, A.J.P. (1968) New determinations of the saturation magnetization of nickel and iron. *Journal of Applied Physics*, 39, 669–670.
- Desai, P.D. (1986) Thermodynamic properties of iron and silicon. *Journal of Physical and Chemical Reference Data*, 15, 967–983.
- Deslattes, R.D., and Henins, A. (1973) X-ray to visible wavelength ratios. *Physical Review Letters*, 31, 972–975.
- Dieckmann, R. (1982) Defects and cation distribution in magnetite (IV): Nonstoichiometry and point defect structure of magnetite ( $\text{Fe}_{1-x}\text{O}_4$ ). *Berichte der Bunsengesellschaft für Physikalische Chemie*, 86, 112–118.
- Fei, Y., and Saxena, S.K. (1986) A thermodynamic data base for phase equilibria in the system Fe-Mg-Si-O at high pressure and temperature. *Physics and Chemistry of Minerals*, 13, 311–324.
- Grønvold, F. (1967) Adiabatic calorimetry for the investigation of reactive substances in the range from 25 to 775 °C: Heat capacity of  $\alpha$ -aluminium oxide. *Acta Chemica Scandinavia*, 21, 1695–1713.
- (1993) Enthalpy of fusion and temperature of fusion of indium, and redetermination of the enthalpy of fusion of tin. *Journal of Chemical Thermodynamics*, 25, 1133–1144.
- Grønvold, F., Stølen, S., Tolmach, P., and Westrum, E.F., Jr. (1993) Heat capacities of the wüstites  $\text{Fe}_{0.9379}\text{O}$  and  $\text{Fe}_{0.9254}\text{O}$  at temperatures from 5 K to 350 K: Thermodynamics of the reaction:  $x\text{Fe}(s) + (1/4)\text{Fe}_3\text{O}_4(s) = \text{Fe}_{0.7500+x}\text{O}(s) = \text{Fe}_{1-x}\text{O}(s)$  at  $T = 850$  K, and properties of  $\text{Fe}_{1-x}\text{O}(s)$  to  $T = 1000$  K. *Journal of Chemical Thermodynamics*, 25, 1089–1117.
- Haas, J.R., Jr., and Hemingway, B.S. (1992) Recommended standard electrochemical potentials and fugacities of oxygen for the solid buffers and thermodynamic data in the systems iron-silicon-oxygen, nickel-oxygen, and copper-oxygen. U.S. Geological Survey, Open File Report 92–267.
- Jeanloz, R. (1990) The nature of the Earth's core. *Annual Reviews of Earth and Planetary Science*, 18, 357–386.
- Knittle, E., and Jeanloz, R. (1989) Simulating the core-mantle boundary: An experimental study of high-pressure reactions between silicates and liquid iron. *Geophysical Research Letters*, 16, 609–612.
- (1991) Earth's core-mantle boundary: Results of experiments at high pressures and temperatures. *Science*, 251, 1438–1443.
- Koch, F.B., and Fine, M.E. (1967) Magnetic properties of  $\text{Fe}_x\text{O}$  as related to the defect structure. *Journal of Applied Physics*, 38, 1470–1471.
- Liu, L. (1975) Post-oxide phases of forsterite and enstatite. *Geophysical Research Letters*, 2, 417–419.
- Mainard, R., Boubel, M., and Fousse, H. (1968) On the specific-heat anomaly in  $\text{Fe}_x\text{O}$ . *Comptes Rendus de l'Académie des Sciences, series B(12)*, 1299–1301 (in French).
- McCammon, C.A. (1992) Magnetic properties of  $\text{Fe}_x\text{O}$  ( $x > 0.95$ ): Variation of Néel temperature. *Journal of Magnetism and Magnetic Materials*, 104–107, 1937–1938.
- (1993) Effect of pressure on the composition of the lower mantle end member  $\text{Fe}_x\text{O}$ . *Science*, 259, 66–68.
- McCammon, C.A., and Liu, L. (1984) The effect of pressure on nonstoichiometric wüstite,  $\text{Fe}_x\text{O}$ : The iron-rich phase boundary. *Physics and Chemistry of Minerals*, 10, 106–113.
- Schweika, W., Hoser, A., Martin, M., and Carlsson, A.E. (1995) Defect structure of ferrous oxide  $\text{Fe}_{1-x}\text{O}$ . *Physical Review B*, 51, 15771–15788.
- Seehra, M.S., and Srinivasan, G. (1984) Magnetic studies of non-stoichiometric  $\text{Fe}_x\text{O}$  and evidence for magnetic clusters. *Journal of Physics C: Solid State Physics*, 17, 883–892.
- Shen, P., Bassett, W.A., and Liu, L. (1983) Experimental determination of the effect of pressure and temperature on the stoichiometry and phase relations of wüstite. *Geochimica et Cosmochimica Acta*, 47, 773–778.
- Shepherd, J.P., Koenitzer, J.W., Aragon, R., Spalek, J., and Honig, J.M. (1991) Heat capacity and entropy of nonstoichiometric magnetite  $\text{Fe}_{3(1-x)}\text{O}_4$ : Thermodynamic nature of the Verwey transition. *Physical Review*, 43, 8461–8471.
- Simons, B., and Seifert, F. (1979) High-pressure wüstite: Cell parameters and Mössbauer spectra. *Annual Report Geophysical Laboratory (Washington, DC)*, 78, 625–626.
- Stølen, S., Glöckner, R., and Grønvold, F. (1995) Nearly stoichiometric iron monoxide formed as a metastable intermediate in a two-stage disproportionation of quenched wüstite—thermodynamic and kinetic aspects. *Thermochemica Acta*, 256, 91–106.
- Sundman, B. (1991) An assessment of the Fe-O system. *Journal of Phase Equilibria*, 12, 127–140.
- Takai, S., Atake, T., and Koga, Y. (1994a) Heat capacity anomalies at the Verwey transition of  $\text{Fe}_{3(1-x)}\text{O}_4$ . *Thermochemica Acta*, 246, 1–10.
- Takai, S., Akishige, Y., Kawaji, H., Atake, T., and Sawaguchi, E. (1994b) Low temperature heat capacities and Verwey transition of magnetite. *Journal of Chemical Thermodynamics*, 26, 1259–1266.
- Todd, S.S., and Bonnicksen, K.R. (1951) Low temperature heat capacities and entropies at 298.15 K of ferrous oxide, manganous oxide and vanadium monoxide. *Journal of the American Chemical Society*, 73, 3894–3895.

MANUSCRIPT RECEIVED AUGUST 14, 1995

MANUSCRIPT ACCEPTED MARCH 20, 1996